Extraction and reconstruction of shape information from a digital hologram of three-dimensional objects

C. P. Mc Elhinney, J. Maycock, B. M. Hennelly, T. J. Naughton, J. B. McDonald
Dept. of Computer Science
National University of Ireland
Maynooth
Co. Kildare , Ireland
conormce@cs.nuim.ie tom.naughton@nuim.ie johnmcd@cs.nuim.ie

B. Javidi
Electrical and Computer Engineering
University of Connecticut
371 Fairfield Road, Unit 1157
Storrs, CT 06269, USA

Abstract

We present a technique to convert a digital hologram of a three-dimensional object into a surface profile of the object. A depth-from-defocus technique is used to generate a depth map for a particular reconstructed perspective of the scene. The Fresnel transform is used to effect defocus. This depth map is then used to create an extended focused image of the object. Through the combination of the extended focused image and the depth map we are able to reconstruct a pseudo three-dimensional representation of the object. Our method produces depth maps of a significantly higher resolution than current autofocus methods. The technique could be used in registration and three-dimensional object recognition applications.

Keywords: digital holography, scene reconstruction, 3D shape measurement, three-dimensional image processing

1 Introduction

Holography [1] is an established technique for recording and reconstructing real-world three-dimensional (3D) objects. Digital holography [2, 3, 4, 5, 6, 7, 8, 9] and digital holographic image processing [9, 10, 11, 12, 13] have recently become feasible due to advances in megapixel CCD sensors with high spatial resolution and high dynamic range. A technique known as phase shift interferometry (PSI) [6, 8] is used to create our in-line digital holograms [9, 10]. The resulting digital holograms are in an appropriate form for data transmission and digital image processing.

Digital holography is one of several possible optical techniques for recovery of shape information [14]. Digital holographic microscopy [15, 16, 17] and interferometric [3] methods use a phase unwrapping approach to obtain the profile of an object. Many existing 3D imaging techniques are based on the explicit combination of several two-dimensional perspectives through digital image processing. Multiple perspectives of a 3D object can be combined optically, in parallel, and stored together as a single complex-valued digital hologram. We apply a technique known as depth-from-defocus (DFD) to create depth maps of the objects encoded in our digital holograms.

Several approaches for focusing digital holograms have been reported in the literature [18, 19, 20]. Two of these approaches attempt to focus the numerically reconstructed complex wave field [18, 19]. Liebling [18] used Fresnelets on holograms captured using digital holographic microscopy [21], to discover the focal plane for an micrometric object, but no shape measurement is attempted. Gillespie and King [19] proposed the use of the self-entropy of a hologram's quantised phase to calculate the sharpness of a numerically reconstructed complex wave field. Another approach is to try to reconstruct the 3D scene using a focus metric calculated on reconstructions of the hologram at different depths. Ma *et al.* [20] used variance to calculate a depth map from a digitised analog hologram. In this paper we extend on our previous work [22] by using non-overlapping blocks to create an extended focused image and a pseudo 3D representation of the hologram.

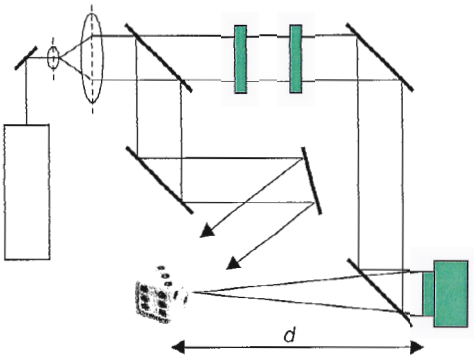

Figure 1: Experimental setup for PSI: BE, beam expander; BS, beam splitter; RP, retardation plate; M, mirror.

In Sect. 2, we describe how 3D objects are captured using phase-shift digital holography. We then describe the experiments involved in extracting a depth map from a digital hologram in Sect. 3. Section 4 details how to reconstruct a pseudo 3D representation of an object encoded in a digital hologram and, finally, conclusions are drawn in Sect. 5.

2 Phase-Shift Digital Holography

We record Fresnel fields with an optical system based on a Mach-Zehnder interferometer (see Fig. 1). A linearly polarised Argon ion (514.5 nm) laser beam is expanded and collimated, and divided into object and reference beams. The object beam illuminates a reference object placed at a distance of approximately $d = 350$ mm from a 10-bit 2028×2044 pixel Kodak Megaplus CCD camera. Let $U_0(x, y)$ be the complex amplitude distribution immediately in front of the 3D object. The linearly polarised reference beam passes through half-wave plate RP_1 and quarter-wave plate RP_2. By selectively removing the plates we can achieve four phase shift permutations of 0, $-\pi/2$, $-\pi$, and $-3\pi/2$. The reference beam combines with the light diffracted from the object and forms an interference pattern in the plane of the camera. At each of the four phase shifts we record an interrogram. We use these four real-valued images to compute the camera-plane complex field $H_0(x, y)$ by PSI [6, 8]. We call this computed field a digital hologram.

A digital hologram $H_0(x, y)$ contains sufficient amplitude and phase information to reconstruct the complex field $U(x, y, z)$ in a plane in the object beam at any distance z from the camera [4, 8, 9]. This can be calculated from the Fresnel approximation [23] as

$$U(x, y, z) = \frac{-\mathrm{i}}{z} \exp\left(\mathrm{i}\frac{2\pi}{}z\right) H_0(x, y) \star \exp\left[\mathrm{i}\pi\frac{(x^2 + y^2)}{z}\right] , \qquad (1)$$

where is the wavelength of the illumination and $\star$ denotes a convolution operation. At $z = d$, and ignoring errors in digital propagation due to discrete space (pixelation) and rounding, the discrete reconstruction $U(x, y, z)$ closely approximates the physical continuous field $U_0(x, y)$.

Furthermore, as with conventional holography [23, 24], a windowed subset of the Fresnel field can be used to reconstruct a particular view of the object. As the window explores the field a different angle of view of the object can be reconstructed. The range of viewing angles is determined by the ratio of the window size to the full CCD sensor dimensions. Our CCD sensor has approximate dimensions of 18.5×18.5 mm and so a 1024×1024 pixel window has a maximum lateral shift of 9 mm across the face of the sensor. With an object positioned $d = 350$ mm from the camera, viewing angles in the range of 1.5 are permitted. Smaller windows will permit a larger range of viewing angles at the expense of image quality at eachviewpoint.

3 Extraction of shape information

It is possible to reconstruct the object wavefield at any depth by altering the distance parameter z of Equation 1. One method for reconstructing a hologram at the most in-focus plane is to use a DFD technique. This is done by reconstructing the hologram over a range of depths and evaluating each 2D image using a focus metric, this will return the in-focus plane's depth. This technique relies on the assumption that a large majority of the scene is in focus at a certain depth. If there are multiple objects

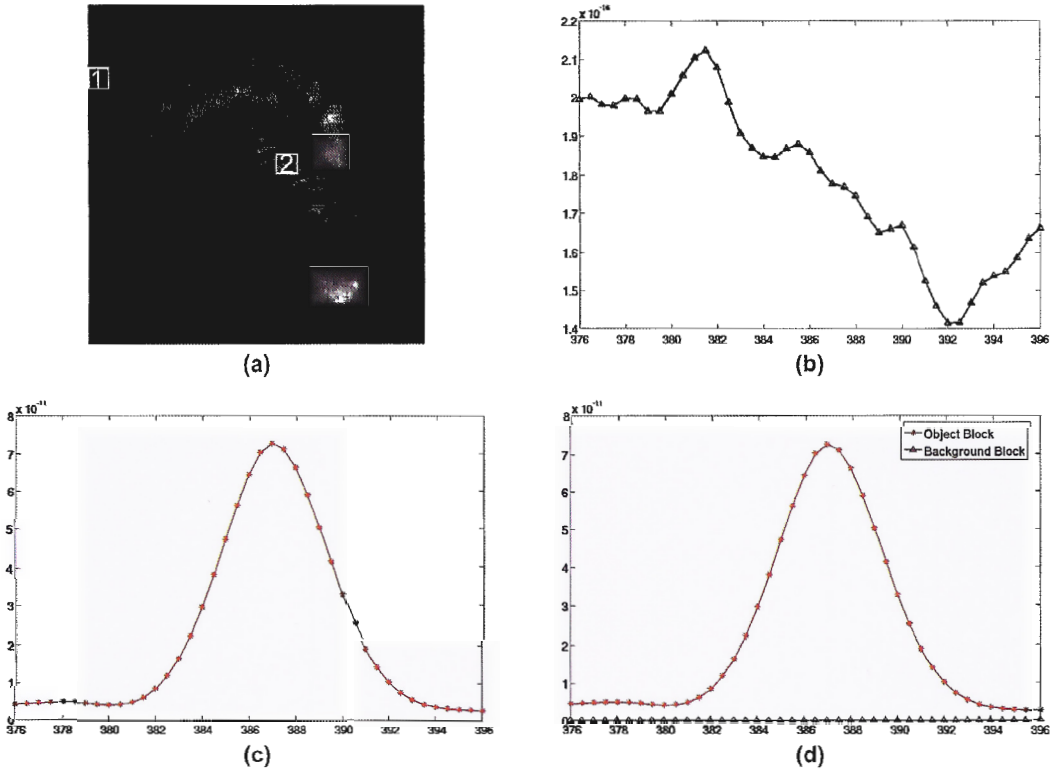

Figure 2: Reconstruction of the bolt,(a), and two trace plots of variance calculated on the amplitude of two blocks, (b) trace plot of block 1 positioned in a background region, (c) trace plot of block 2 positioned on the threads of the bolt, (d) both trace plots plotted on the same scale.

at different depths, or if the object is not relatively smooth, the scene needs to be partitioned into blocks. Each block can then be processed using a focus metric in order to gather depth information. This depth information can then be used to create a depth-map of the scene.

An approach for the recovery of shape information from digital holograms was proposed by Ma [20]. He uses variance as a focus metric to gather depth information from a digital hologram. This is defined as,

$$V(k) = \frac{1}{n \times n} \sum_{i=1}^{n} \sum_{j=1}^{n} \left[I_k(i,j) - \overline{I_k} \right]^2 \tag{2}$$

where I_k is the k^{th} block in the image and $\overline{I_k}$ is the mean of the input block. Through block processing of the complex wave field and the calculation of variance on these blocks, depth maps have been successfully created from digitally scanned material holograms. We were the first to apply this technique to digitally captured holograms [22].

Our holograms are reconstructed at a set of different depths L using Equation 1, starting at a depth d_0. All our reconstructions have had a selected speckle reduction technique applied to them [25]. The size of each reconstruction is $M \times N$ with Δz being the interval between reconstructions. We calculate the focus at each depth by separating each reconstruction into blocks of size $n \times n$, creating $m' \times n'$ blocks. Each of these blocks are then processed using variance as a focus metric. The estimated depth for each block is evaluated by finding the depth at which variance exhibits a maximum. This gives us the shape information we need in the form of a depth map, where each value in the depth map represents the distance from the hologram plane to the corresponding block in the scene.

3.1 Non-Overlapping Blocks Approach

Depth maps created using the approach described above can suffer from noise introduced by the estimation of depths in background regions and incorrect estimation of depth in object regions. A reconstruction of the bolt hologram is shown in Fig. 2(a), the two labelled blocks are an object block and a background block. Trace plots for variance calculated on these blocks are shown for the background block in Fig. 2(b), and for the object block in Fig.2(c). In Fig. 2(d) we have plotted the two trace plots on the same scale, it is clear that variance calculated on the background block returns a lower value than

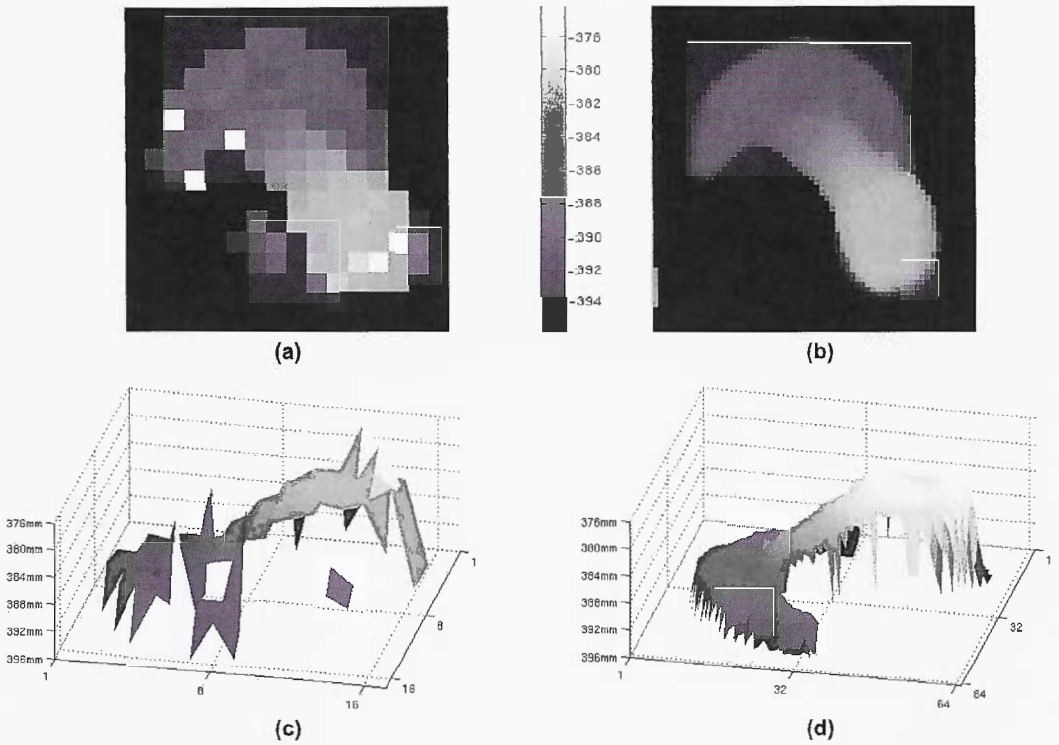

Figure 3: 2D depth maps acquired with (a) a 64×64 block size, (b) a 16×16 block size. Surface plots of the depth maps acquired with (c) a 64×64 block size, (d) a 16×16 block size.

that for the object region, in the order of 10^{5} less. We found this to be true in the general case and used this to threshold our depth maps and remove depth estimations relating to background regions.

We first extracted shape information from a digital hologram using non-overlapping blocks [22]. This resulted in depth maps which were $\frac{M}{n} \times \frac{N}{n}$ in size. We reconstructed a hologram of a bolt forty different depths ($L = 40$), with $0.5mm$ intervals ($\Delta z = 0.5$mm) and starting at a depth of $376mm$ ($d_0 = 376$mm). The resolution of the reconstructions are 1024×1024 pixels. It was necessary to experiment with different blocks sizes to determine what the impact of larger or smaller block sizes on the depth map would be. A reduction in block size can improve the definition of features in the depth map. At some threshold point this leads to more discontinuities in the depth map. This behaviour at the threshold point is scene dependent. The discontinuities manifest themselves as both holes and spikes, which means a larger closing operation is required thus reducing the overall accuracy of the depth map. We have found that using block sizes of less than 16×16 leads to a high proportion of holes and spikes in the depth map due to the presence of speckle in the reconstructions. This high quantity of holes and spikes require more post-processing of the depth map then is required for larger block sizes and leads to an overally smoothed depth map. The depth maps acquired through calculating variance on the bolt hologram with two different block sizes are shown in Fig. 3. Figure 3(a) shows an image representation of a depth map acquired using a 64×64 block size and Fig. 3(b) shows a surface plot of this depth map. The white spots that can be seen in Fig. 3(a) are blocks whose depth has been incorrectly estimated, through median filtering these blocks are capable of being suppressed. However, no median filtering was applied to this depth map due its destructive impact on the depth map. When we reduced the block size to 16×16, it was necessary to median filter the depth map in order to suppress error caused by the lower block size. The depth map and surface plot shown in Fig. 3(b) and (c) have been median filtered with a 9×9 filtering neighbourhood. Two of the main regions in the bolt are the front of the bolt and the back of the bolt. As can be seen from Fig. 3, these are being focused at the correct depths of 390mm and 382mm, respectively.

3.2 Overlapping Blocks Approach

In order to create depth maps with an improved resolution we attempted to use variance calculated on overlapping blocks. This would increase the resolution of our depth maps from $\left(\frac{M}{n}\right) \times \left(\frac{N}{n}\right)$, using a non-overlapping approach, to $(M - n) \times (N - n)$. This increased resolution significantly improves the quality of our depth map. This improvement is most visible in the threaded region of the bolt, and also

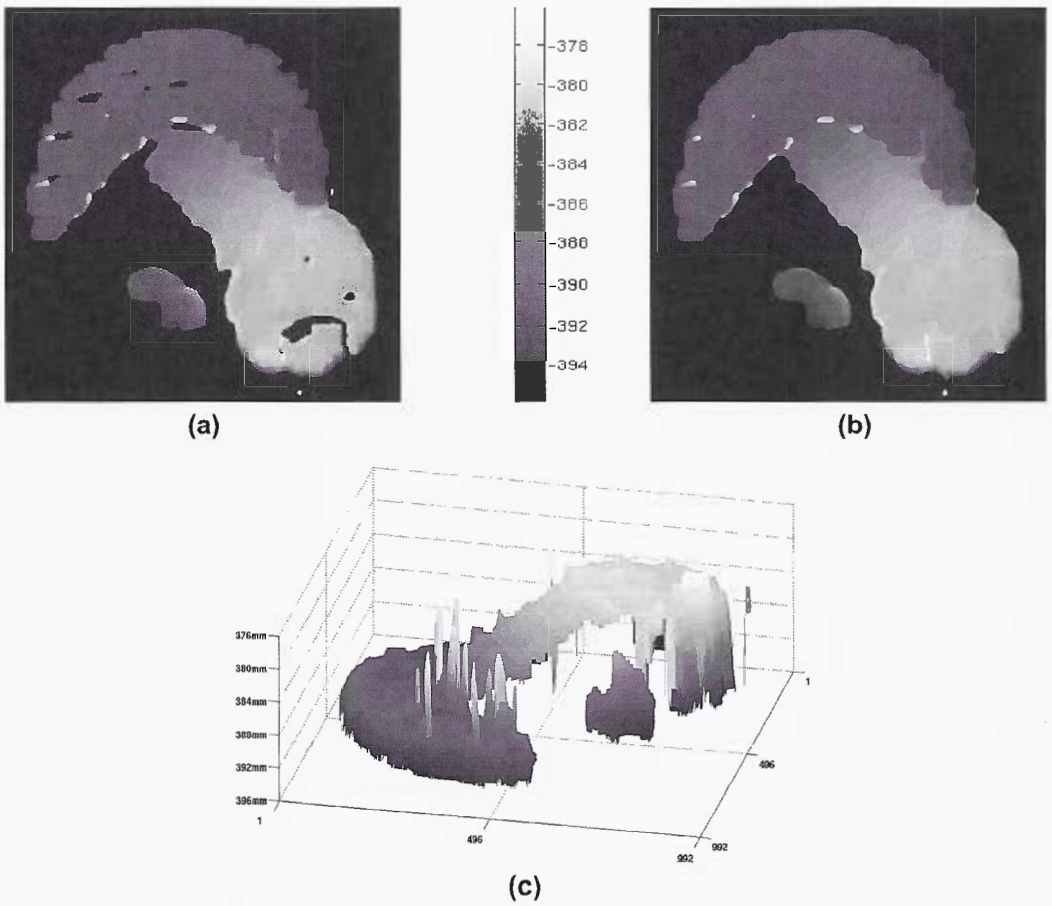

Figure 4: 2D depth maps acquired using a 64×64 block size (a) prior to closing, (b) after closing and (c) a surface plot of the depth map.

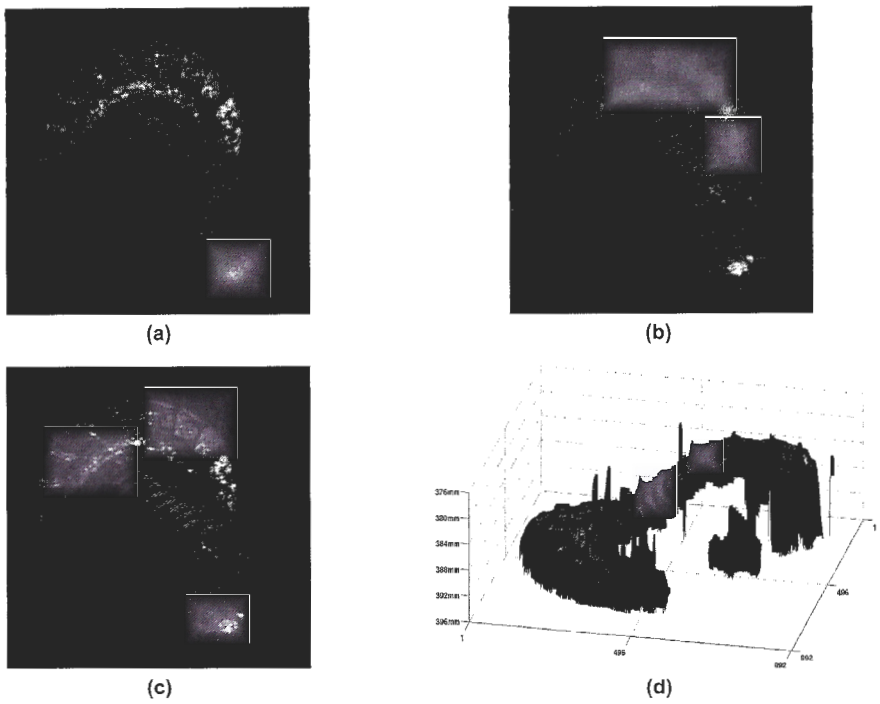

Figure 5: Reconstructions of the bolt hologram, (a) reconstruction of the bolt with the back in focus, (b) reconstruction of the bolt with the front in focus, (c) extended focus image and (d) psueod 3D representation of the bolt.

on the back face of the bolt which is not perpendicular to the optical axis. On a 3Ghz Pentium PC with 1GB of RAM, using a 64×64 block size, it takes less than 3 hours to run this technique. The results of using variance as a focus metric with a 64×64 block size using an overlapping approach can be seen in Fig. 4.

We applied median filtering with a neighbourhood of 15×15 to the depth map, as shown in Fig. 4(a). Some object regions in the depth map were incorrectly removed after thresholding was applied. We used a mathematical morphological closing operation on the depth map using a disk structuring element with a 25 pixel diameter to fill in the holes in the image. The resultant depth map can be seen in Fig. 4(b), and the surface plot of this depth map is shown in Fig. 4(c). Some blocks have not had their depth correctly estimated, as can be seen in Fig. 4(c). It is our hope that through the evaluation of different focus metrics we will reduce the number of these blocks such that combination of median filtering and closing will suppress them. Both median filtering and the closing operation are destructive error suppression and error removal techniques. Therefore, median filtering and closing have the effect of smoothing the data, this can remove details in the original depth map. We note that the increased resolution given through using an overlapping approach produces depth maps with much greater detail.

4 Scene Reconstruction of three-dimensional objects

With the increased resolution obtained through using a overlapping block approach, we are able to use our depth map to create an image with an extended depth of field encompassing the whole object. This is an image where each pixel in the image is in-focus. This is one major advantage of using an overlapping block approach over the non-overlapping approach. Our non-overlapping block experiments produced depth maps of size 16×16 and 64×64, only allowing for an extended focused image of that size. However, using the overlapping approach the extended focused image produced was 960×960 pixels.

To create the extended focused image we use L reconstructions and a depth map. Each pixel location (i, j) in the depth map contains a depth value d . Our extended focused image copies the value from position (i, j) in the reconstruction obtained at depth d. Figure 5(a) and Fig. 5(b) show two reconstructions of the bolt hologram in which the back of the bolt and the front of the bolt are in focus, respectively. The extended focused image is shown in Fig. 5(c). This extended focused image also verifies, qualita-

tively, that our depth maps are calculating the correct depth. If an incorrect depth had been calculated, the object, or large regions of the object, would be blurred in the extended focused image. Figure 5(d) shows a pseudo 3D representation of the object obtained through the combination of the depth map and the extended focused image.

5 Conclusion

We have presented a technique for extracting shape information from a digital hologram. We have shown depth maps created by this technique, using two different approaches on a digital hologram of a bolt. We have demonstrated that an overlapping block approach is superior to a non-overlapping approach due to its increased resolution. This increased resolution gives us a more accurate depth map and it also, significantly, allows us to create an extended focused image of the object and create a pseudo three-dimensional representation of the object. Our technique might be applicable in situations where the object has too large a depth range, too rough of a surface, or is captured at too low a resolution for other techniques such as phase unwrapping to work adequately but may only be appropriate for objects with slow-varying depth. Using reconstructions with a smaller interval between them would result in a more accurate depth map. In the presentation we will demonstrate experimental results using other digital holograms and scenes. We intend to extend this technique through quantitative measurement of known objects to measure the accuracy of our approach, and to develop non-destructive error removal techniques.

Acknowledgements

The authors wish to thank Enrique Tajahuerce and Yann Frauel for use of their digital hologram data. Support is acknowledged from Enterprise Ireland and Science Foundation Ireland.

References

[1] D. Gabor. A new microscope principle. *Nature*, 161:77–79, 1948.

[2] J. W. Goodman and R. W. Lawrence. Digital image formation from electronically detected holograms. *Applied Physics Letters*, 11:77–79, 1967.

[3] T. Kreis. *Handbook of Holographic Interferometry*. Optical and Digital Methods, Wiley-Vch, Weinheim, 2005.

[4] L. Onural and P. D. Scott. Digital decoding of in-line holograms. *Opt. Eng.*, 26:1124–1132, 1987.

[5] L. P. Yaroslavskii and N. S. Merzlyakov. *Methods of Digital Holography*. Consultants Bureau, New York, 1980. Translated from Russian by Dave Parsons.

[6] J. H. Bruning, D. R. Herriott, J. E. Gallagher, D. P. Rosenfeld, A. D. White, and D. J. Brangaccio. Digital wavefront measuring interferometer for testing optical surfaces and lenses. *Applied Optics*, 13:2693–2703, 1974.

[7] U. Schnars and W. P. O. Jüptner. Direct recording of holograms by a ccd target and numerical reconstruction. *Applied Optics*, 33:179–181, 1994.

[8] I. Yamaguchi and T. Zhang. Phase-shifting digital holography. *Optics Letters*, 22:1268–1270, 1997.

[9] B. Javidi and E. Tajahuerce. Three-dimensional object recognition by use of digital holography. *Optics Letters*, 25:610–612, 2000.

[10] Y. Frauel, E. Tajahuerce, M.-A. Castro, and B. Javidi. Distortion-tolerant three-dimensional object recognition with digital holography. *Applied Optics*, 40:3887–3893, 2001.

[11] T. J. Naughton, Y. Frauel, B. Javidi, and E. Tajahuerce. Compression of digital holograms for three-dimensional object reconstruction and recognition. *Applied Optics*, 41:4124–4132, 2002.

[12] O. Matoba, T. J. Naughton, Y. Frauel, N. Bertaux, and B. Javidi. Real-time three-dimensional object reconstruction by use of a phase-encoded digital hologram. *Applied Optics*, 41:6187–6192, 2002.

[13] J. Maycock, C. P. McElhinney, B. M. Hennelly, T. J. Naughton, J. B. McDonald, and B. Javidi. Reconstruction of partially occluded objects encoded in three-dimensional scenes by using digital holograms. *Applied Optics*, 45:2975–2985, 2006.

[14] F. Chen, G. Brown, and M. Song. Overview of three-dimensional shape measurement using optical methods. *Optical Engineering*, 39:10–22, 2000.

[15] P. Ferraro, S. Nicola, G. Coppolla, A. Finizio, D. Alfieri, and G. Pierattini. Controlling image size as a function of distance and wavelength in fresnel-transform reconstruction of digital holograms. *Optics Letters*, 29:854–856, 2004.

[16] P. Ferraro, S. Grilli, D. Alfrieri, S. Nicola, A. Finizio, G. Pierattini, B. Javidi, G. Coppolla, and V. Striano. Extended focused image in microscopy by digital holography. *Optics Express*, 13:6738–6749, 2005.

[17] T. Zhang and I. Yamaguchi. Three-dimensional microscopy with phase-shifting digital holography. *Optics Letters*, 23:1221–1223, 1998.

[18] M. Liebling and M. Usner. Autofocus for digital fresnel holograms by use of a Fresnelet-sparsity criterion. *J. Opt. Soc Am. A*, 21:2424–2430, 2004.

[19] J. Gillespie and R. King. The use of self-entropy as a focus measure in digital holography. *Pattern Recognition Letters*, 9:19–25, 1989.

[20] L. Ma, H. Wang, Y. Li, and H. Jin. Numerical reconstruction of digital holograms for three-dimensional shape measurement. *Journal of Optics A*, 6:396–400, 2004.

[21] T. Colomb, E. Cuche, P. Dahlgen, A. Marian, F. Montfort, C. Depeursinge, P. Marquet, and P. Magistretti. 3D imaging of surfaces and cells by numerical reconstruction of wavefronts in digital holography applied to transmission and reflection microscopy. *Proc. IEEE - International Symposium on Biomedical Imaging*, pages 773–776, 2002.

[22] C. P. McElhinney, J. Maycock, T. J. Naughton, J. B. McDonald, and B. Javidi. Extraction of three-dimensional shape information from a digital hologram. *Proc. SPIE*, 5908:30–41, 2005.

[23] J. W. Goodman. *Introduction to Fourier Optics*. Roberts and Company, Englewood, Colorado, third edition, 2005.

[24] H. J. Caulfield. *Handbook of Optical Holography*. Academic Press, New York, 1979.

[25] J. Maycock, B. M. Hennelly, J. B. McDonald, T. J. Naughton, Y. Frauel, A. Castro, and B. Javidi. Reduction of speckle in digital holography by discrete fourier filtering. *submitted to Opt. Lett.*, 2006.